Bull. Nov. Comp. Center, Num. Model. in Atmosph., etc., 15 (2015), 51–65

Modeling of the nonlinear motion of saturated granular media*

Yu.V. Perepechko, K.E. Sorokin, Kh.Kh. Imomnazarov

Abstract. A nonlinear model of the saturated granular media based on a two-phase mixture model of viscous liquids is proposed. A mathematical model of the two-velocity dynamics of a granular medium involves the temperature phase equilibrium and the absence of the pressure phase equilibrium and is consistent from the thermodynamic standpoint. The obtained two-velocity model was verified by comparison with the results of numerical calculations for the one-velocity model. The convective and the pressure flows of the mixture of compressible viscous liquids for various conditions are simulated.

Introduction

In this paper, the nonlinear hydrodynamics of saturated granular media is investigated. Published works on this topic are focused, mainly, on the investigation of acoustic processes in multiphase media or on the large-scale study of the two-fluid hydrodynamics of incompressible media. Heat and mass transfer processes in compressible saturated granular media for a wide range of time periods have been studied to a lesser extent. Complexity of the experimental verification of numerical modeling of such systems requires the use of both mathematical and numerical methods to ensure the correctness of the physical model of differential equations and their finite difference approximation.

The mathematical model developed in this paper is constructed within the framework of conservation laws method [1, 2]. The method is based on matching the first and second laws of thermodynamics, conservation laws, and group invariance of the equations, which provides the thermodynamic consistency of nonlinear dynamics models of complex subsurface geometries. With this approach we have obtained various models of the dynamics of a two-velocity medium: saturated porous media [2–4], two-fluid media both assuming the phase pressure equilibrium [5] and without it [6]. The comparison of the simulation results for the model of saturated porous media [7] with experimental data on the Stoneley wave [8] demonstrated the efficacy of the method of conservation laws for classical simulations of complex media.

*Supported by the RFBR under Grant 13-01-00689, The Russian Ministry of Education under Grant (HA-07.514.11.4156).

1. Mathematical model

The model of the two-phase medium, studied in this paper, assumes the absence of the pressure equilibrium between the phases, but the presence of the temperature equilibrium [5]. The two-velocity medium has the following structure: solid granules move relative to the fluid, interacting both directly, and through the fluid. Solids and fluids jointly make up a two-velocity continuum whose unit volume is characterized by two densities, two velocities, and entropy. The choice of the functional dependence of the internal energy fixes thermodynamics of the medium: the internal energy per unit volume of the medium is determined by the first law of thermodynamics:

$$dE_0 = T\,dS + \mu\,d\rho + q\,d\rho_1 + (\boldsymbol{u} - \boldsymbol{v}, d\boldsymbol{j}_0), \tag{1}$$

where ρ, ρ_1, ρ_2 are the density of the medium, the partial density of solid granules and the partial density of the fluid, respectively, $\rho = \rho_1 + \rho_2$, μ is the chemical potential, q is the potential of interfacial interaction, E_0 is the internal energy per unit volume, S is the entropy per unit volume, T is the temperature, $\boldsymbol{u}$ is the granule velocity, $\boldsymbol{v}$ is the fluid velocity, $\boldsymbol{j}_0 = \boldsymbol{j} - \rho\boldsymbol{v}$ is part of the momentum density which is invariant in terms of the Galilei transformations, and $\boldsymbol{j} = \rho_1\boldsymbol{u} + \rho_2\boldsymbol{v}$ is the momentum density.

The evolution of the density of the two-phase medium and of the granule density is determined by the conservation laws

$$\frac{\partial\rho}{\partial t} + \operatorname{div}\boldsymbol{j} = 0, \quad \frac{\partial\rho_1}{\partial t} + \operatorname{div}(\rho_1\boldsymbol{u}) = 0. \tag{2}$$

The mass conservation law of the fluid is a consequence of equations (2).

The laws of conservation of momentum, energy, entropy (in reversible approximation) should also be valid

$$\frac{\partial j_i}{\partial t} + \partial_k\Pi_{ik} = 0 \ \ (i = 1, 2, 3), \quad \frac{\partial E}{\partial t} + \operatorname{div}\boldsymbol{Q} = 0, \quad \frac{\partial S}{\partial t} + \operatorname{div}\Big(\frac{S}{\rho}\boldsymbol{j}\Big) = 0. \tag{3}$$

Here and after the summation from 1 to 3 is carried out in terms of the repeated indices, $\partial_i = \frac{\partial}{\partial x_i}$, Π_{ik} is the momentum flux density tensor, $E = E_0 + (\boldsymbol{v}, \boldsymbol{j}_0) + \rho\boldsymbol{v}^2/2$ is the total energy per unit volume, $\boldsymbol{Q}$ is the flux of energy, and S is the entropy per unit volume.

The system of equations (2) and (3) needs to be supplemented with the equation of motion of one of the phases, in this case with the equation of fluid [2]

$$\frac{\partial\boldsymbol{v}}{\partial t} + (\boldsymbol{v}, \nabla)\boldsymbol{v} = -\nabla\mu - \frac{S}{\rho}\nabla T, \tag{4}$$

in which the kind of forces causing the motion of the fluid is determined by the conditions of fulfilment of thermodynamic equilibrium: $\nabla\mu = 0$, $\nabla T = 0$, $\boldsymbol{u} = \boldsymbol{v}$.

The fluxes and pressure in the medium are uniquely determined in the process of implementation of the conservation laws [5]

$$\begin{aligned} \boldsymbol{Q} &= \Big(\mu + \frac{v^2}{2} - (\boldsymbol{u},\boldsymbol{v})\Big)\boldsymbol{j} + TS\frac{\boldsymbol{j}}{\rho} + (\boldsymbol{u}, \boldsymbol{j} - \rho\boldsymbol{v})\boldsymbol{u} + q\rho_1\boldsymbol{u}, \\ \Pi_{ik} &= \rho_1 u_i u_k + \rho_2 v_i v_k + p\delta_{ik} + q\rho_1\delta_{ij}, \\ p &= -E_0 + TS + \mu\rho + (\boldsymbol{u} - \boldsymbol{v}, \boldsymbol{j} - \rho\boldsymbol{v}). \end{aligned} \tag{5}$$

The presence of the direct interaction of granules leads to an additional contribution to the internal energy (the term $q\,d\rho_1$) and, as a consequence, additional contributions to the flux of energy and the momentum flux density tensor. The stress tensor is defined in the ordinary way $\sigma_{ik} = -p\delta_{ik} - q\rho_1\delta_{jk}$.

Inclusion of dissipative processes leads to additional fluxes in the governing equations

$$\frac{\partial E}{\partial t} + \partial_i(Q_i + W_i) = 0, \tag{6}$$

$$\frac{\partial j_i}{\partial t} + \partial_k(\Pi_{ik} + \pi_{1ik} + \pi_{2ik}) = 0. \tag{7}$$

Here the fluxes $\boldsymbol{Q}$ and Π_{ik} are defined by (5), $\boldsymbol{W}$ is the irreversible energy flux, π_{1ik}, π_{2ik} are the irreversible momentum fluxes. The friction force of the interfacial friction $\boldsymbol{f}$ should be introduced into the equation of motion of the continuum fluid:

$$\frac{\partial \boldsymbol{v}}{\partial t} + (\boldsymbol{v}, \nabla)\boldsymbol{v} = -\frac{1}{\rho}\nabla p + \frac{\rho_1}{\rho}\nabla q + \boldsymbol{f}. \tag{8}$$

The entropy flux $\boldsymbol{f}_q$ and the entropy production R are added into the equation for entropy

$$\frac{\partial S}{\partial t} + \operatorname{div}\Big(\frac{S}{\rho}\boldsymbol{j} + \boldsymbol{f}_q\Big) = \frac{R}{T}. \tag{9}$$

The procedure of matching equations (2), (6)–(9) with the first law of thermodynamics (1) leads to the definition of the energy flux and, according to the Onsager theory, to the dissipation function as well [2]

$$W_i = q_i + \pi_{1ik}u_k + \pi_{2ik}v_k, \quad R = \boldsymbol{f}(\boldsymbol{u}_1 - \boldsymbol{u}_2) + \boldsymbol{f}_q\nabla T + \pi_{1ik}u_{ik} + \pi_{2ik}v_{ik}.$$

The structure of the dissipation function allows one to enter the linear dissipation relations for the fluxes of the vector nature and their corresponding thermodynamic forces.

The two-velocity two-fluid dynamics equations with thermodynamics of the medium, specified by the dependence $e = e(\rho_1, \rho_2, \boldsymbol{u}, \boldsymbol{v}, s)$, can be represented in a gravitational field as

$$\frac{\partial \rho_1}{\partial t} + \operatorname{div}(\rho_1 \boldsymbol{u}) = 0, \qquad \frac{\partial \rho_2}{\partial t} + \operatorname{div}(\rho_2 \boldsymbol{v}) = 0, \tag{10}$$

$$\frac{\partial \boldsymbol{u}}{\partial t} + (\boldsymbol{u}, \nabla)\boldsymbol{u} = -\frac{1}{\rho}\nabla p - \frac{\rho_2}{\rho}\nabla q - \frac{\rho_2}{\rho_1}\boldsymbol{f} + \boldsymbol{f}_1 + \boldsymbol{g}, \tag{11}$$

$$\frac{\partial \boldsymbol{v}}{\partial t} + (\boldsymbol{v}, \nabla)\boldsymbol{v} = -\frac{1}{\rho}\nabla p + \frac{\rho_1}{\rho}\nabla q + \boldsymbol{f} + \boldsymbol{f}_2 + \boldsymbol{g}. \tag{12}$$

The entropy is carried by an average velocity of the two-phase flux $\boldsymbol{j}/\rho$:

$$\frac{\partial s}{\partial t} + \frac{1}{\rho}(\boldsymbol{j}, \nabla)s = -\frac{1}{\rho}\operatorname{div} \boldsymbol{f}_q + \frac{R}{\rho T}, \tag{13}$$

where the dissipation function R is determined by

$$R = \rho_2 b(\boldsymbol{u} - \boldsymbol{v})^2 + \kappa \frac{1}{T}(\nabla T)^2 + 2\nu\big(\nabla T, (\boldsymbol{u} - \boldsymbol{v})\big) + \eta_1 u_{ik}^2 + \eta_2 v_{ik}^2. \tag{14}$$

The dissipative fluxes $\boldsymbol{f}$, $\boldsymbol{f}_q$, $\boldsymbol{f}_1$, $\boldsymbol{f}_2$ are defined by the relations

$$\boldsymbol{f} = b(\boldsymbol{u} - \boldsymbol{v}) + \frac{1}{\rho_2}\nu\nabla T, \qquad \boldsymbol{f}_q = \kappa\frac{1}{T}\nabla T + \nu(\boldsymbol{u} - \boldsymbol{v}), \tag{15}$$

$$f_{1i} = \frac{1}{\rho_1}\partial_k(\eta_1 u_{ik}) + \frac{1}{\rho_1}\nu\partial_i T, \qquad f_{2i} = \frac{1}{\rho_2}\partial_k(\eta_2 v_{ik}) - \frac{1}{\rho_2}\nu\partial_i T. \tag{16}$$

Here $u_{ik} = \frac{1}{2}\Big(\partial_k u_i + \partial_i u_k - \frac{2}{3}\delta_{ik}\operatorname{div}\boldsymbol{u}\Big)$, $v_{ik} = \frac{1}{2}\Big(\partial_k v_i + \partial_i v_k - \frac{2}{3}\delta_{ik}\operatorname{div}\boldsymbol{v}\Big)$ are the strain rate tensors; $\boldsymbol{g}$ is the acceleration of gravity, $e = E/\rho$ is the mass energy density, $s = S/\rho$ is the mass entropy density. The interfacial friction coefficient b, the shear viscosities η_i, the thermal conductivity κ and the kinetic coefficient ν are functions of the thermodynamic parameters. Effects of the bulk viscosity are not considered in this paper. The presence of the interphase interaction parameter q, introducing the second pressure into the two-fluid medium, leads, as in porous media, to the appearance of the second longitudinal sound [6].

The equations of state of the two-phase medium closing the dynamic equations (10)–(16) are presented in the linear approximation as follows:

$$\delta\rho_1 = \rho_1\alpha\,\delta p + \rho_1\rho_2\alpha_q\,\delta q - \rho_1\beta\,\delta T,$$
$$\delta\rho_2 = \rho_2\alpha\,\delta p - \rho_1\rho_2\alpha_q\,\delta q - \rho_2\beta\,\delta T.$$

Due to the above assumptions, the total density of the medium and the entropy density are determined only by the temperature and pressure, and do not depend on the second pressure:

$$\delta s = \frac{c_p}{T}\delta T - \frac{1}{\rho}\beta\,\delta p.$$

The introduced coefficients of the volume compression α, α_q, the thermal expansion β, and the specific heat c_p of the two-fluid medium should be determined experimentally. In this model, these coefficients were taken to be additive subsystems. The coefficients of the volumetric compression are associated with the sound velocities in the medium c_1, c_2, by the relations $\alpha^{-1} = \rho c_1^2$, $\alpha_q^{-1} = \rho c_2^2$.

2. Method for solving equations of the model

The solution to nonlinear 2D equations of the two-fluid hydrodynamics without phase pressure equilibrium (10)–(16) was carried out numerically by the control volume method [9]. The numerical solution of the two-velocity hydrodynamics equations (10)–(13) is complicated by the presence of the second pressure in the equations of motion of phases. In order to overcome this problem, the iterative algorithm SIMPLE was adapted to the calculation of pressure fields through corrections in pressures and velocities [10]. For solving a SLAE of a complex structure arising in the equations for the corrections in the pressures, an adapted method of alternating directions, to ensure a rapid convergence of the iterative procedure for dense grids, was used. The calculation results reveal a good convergence of the numerical method.

The scheme of numerical analysis includes the following steps: constructing a grid in the computational domain; discretization of differential equations and boundary conditions, solving a system of linear algebraic equations of discrete analogs; constructing an algorithm for the calculation of the pressure field that is coordinated with the velocity field. The control volume method (CVM) allows obtaining discrete analogs of the original equations of the model that meet the exact integral balances even on coarse meshes. All the numerical calculations of the problems being solved in the two-velocity hydrodynamics are carried out on rectangular uniform grids with a shift of calculation nodes for the components of the velocity vectors (the grids s^1, s^2) with respect to the calculation nodes for other variables in the model (the grid s^0), thus excluding obtaining non-physical solutions (Figure 1). The values of the model variables at a time step are calculated

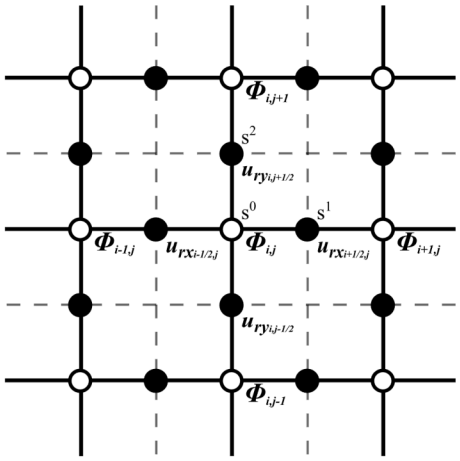

Figure 1. Control volume for the 2D simulation

according to a fully implicit scheme, which allows one to get rid of restrictions on the time step imposed by the Courant condition and makes possible to carry out calculations on the time scales required for applications under consideration.

In discretization of convective terms, in order to determine the values of a dependent variable on the faces of the control volumes we use the scheme with differences opposite to the flux, which provides only the first order approximation of the original equations, however, has a strict physical basis and enables obtaining meaningful solutions in terms of physics in the study of essentially all flux regimes. The result of integration over the control volume (the grid s^1) of the first convective term in the equation of motion will be as follows (here and after $r = 1, 2$):

$$\int_{t^n}^{t^{n+1}} \int_{y_{j-1/2}}^{y_{j+1/2}} \int_{x_i}^{x_{i+1}} u_{rx} \frac{\partial(\rho_r u_{rx})}{\partial x}\, dx\, dy\, dt$$
$$= \Big\{ u^{n+1}_{rx;i+1/2,j} \big[a^1_{i+3/2,j} + a^1_{i-1/2,j} + \big((\rho_r u_{rx})^{n+1}_{i+1,j} - (\rho_r u_{rx})^{n+1}_{i,j} \big) \Delta y \big] -$$
$$u^{n+1}_{rx;i+3/2,j} a^1_{i+3/2,j} - u^{n+1}_{rx;i-1/2,j} a^1_{i-1/2,j} \Big\} \Delta t,$$

where

$$a^1_{i+3/2,j} = \max\Big(-(\rho_r u_{rx})^{n+1}_{i+1,j}, 0 \Big) \Delta y, \quad a^1_{i-1/2,j} = \max\Big((\rho_r u_{rx})^{n+1}_{i,j}, 0 \Big) \Delta y.$$

For the approximation on the faces of control volumes of coefficients, which are part of the diffusion terms of the governing equations, the assumption of a linear variation of such coefficients between the nodes of the computational grid is used. When integrating the diffusion terms as they are, the differences rearward are used. The integration of the first diffusion term of the equation of motion gives

$$\int_{t^n}^{t^{n+1}} \int_{y_{j-1/2}}^{y_{j+1/2}} \int_{x_i}^{x_{i+1}} \frac{\partial}{\partial x} \left(\eta_r \frac{\partial u_{rx}}{\partial x} \right) dx\, dy\, dt$$
$$= \left\{ \eta_{r;i+1,j} \left(\frac{\partial u_{rx}}{\partial x} \right)^{n+1}_{i+1,j} - \eta_{r;i,j} \left(\frac{\partial u_{rx}}{\partial x} \right)^{n+1}_{i,j} \right\} \Delta y\, \Delta t$$
$$= \Big\{ -u^{n+1}_{rx;i+1/2,j} (a^2_{i+3/2,j} + a^2_{i-1/2,j}) + u^{n+1}_{rx;i+3/2,j} a^2_{i+3/2,j} +$$
$$u^{n+1}_{rx;i-1/2,j} a^2_{i-1/2,j} \Big\} \Delta t, \tag{17}$$

where $a^2_{i+3/2,j} = \eta_{r;i+1,j} \dfrac{\Delta y}{\Delta x}$, $a^2_{i-1/2,j} = \eta_{r;i,j} \dfrac{\Delta y}{\Delta x}$.

In integrating the non-stationary terms, as well as the terms taking into account the effect of interfacial interaction and the pressure derivatives the differences rearward are used.

It should be noted that the continuity equation is integrated, but is not explicitly solved. Its resulting discrete analog (the grid s^0):

$$\frac{(\rho_{r;i,j}^{n+1}-\rho_{r;i,j}^{n})\Delta x\Delta y}{\Delta t}+\Big((\rho_r u_{rx})_{i+1/2,j}^{n+1}-(\rho_r u_{rx})_{i-1/2,j}^{n+1}\Big)\Delta y+\Big((\rho_r u_{ry})_{i,j+1/2}^{n+1}-(\rho_r u_{ry})_{i,j-1/2}^{n+1}\Big)\Delta x=0 \tag{18}$$

is used when deriving discrete analogs of other governing equations and when deriving equations for corrections for the pressure and the parameter Q.

After integration of all the terms, the discrete analog of the equation of motion for u_{rx} has the following form:

$$a_{r;i+1/2,j}u_{rx;i+1/2,j}^{n+1}=a_{r;i+3/2,j}u_{rx;i+3/2,j}^{n+1}+a_{r;i-1/2,j}u_{rx;i-1/2,j}^{n+1}+a_{r;i+1/2,j+1}u_{rx;i+1/2,j+1}^{n+1}+a_{r;i+1/2,j-1}u_{rx;i+1/2,j-1}^{n+1}+(-1)^r\frac{\rho_{1;i+1/2,j}^{n+1}\rho_{2;i+1/2,j}^{n+1}}{\rho_{i+1/2,j}^{n+1}}(Q_{i,j}^{n+1}-Q_{i+1,j}^{n+1})\Delta y+\frac{\rho_{r;i+1/2,j}^{n+1}}{\rho_{i+1/2,j}^{n+1}}(P_{i,j}^{n+1}-P_{i+1,j}^{n+1})\Delta y+b_{r;i+1/2,j},$$

$$a_{r;i+3/2,j}=a_{i+3/2,j}^{1}+a_{i+3/2,j}^{2},$$

$$a_{r;i+1/2,j}=a_r^n+a_{r;i+3/2,j}+a_{r;i-1/2,j}+a_{r;i+1/2,j+1}+a_{r;i+1/2,j-1}+b\rho_{2;i+1/2,j}^{n+1}\Delta x\Delta y,$$

$$a_r^n=\frac{\rho_{ri+1/2,j}^{n}\Delta x\Delta y}{\Delta t},$$

$$b_{r;i+1/2,j}=a_r^n u_{rx;i+1/2,j}^n+b\rho_{2;i+1/2,j}^{n+1}u_{(3-r)x;i+1/2,j}^{n+1}\Delta x\Delta y+\tau_{r;i+1/2,j},$$

where $a_{r;i-1/2,j}$, $a_{r;i+1/2,j+1}$, and $a_{r;i+1/2,j-1}$ are calculated similar to $a_{r;i+3/2,j}$, and $\tau_{r;i+1/2,j}$ is the result of integration of cross diffusion terms similar to equation (17). A similar technique is used for discretization of the remaining equations of the model.

This paper investigates hydrodynamic problems whose formulation involves two types of boundary conditions for the equations of motion and for the entropy balance equation, when on the boundary either the values of the dependent variable are specified or the infinity is interpreted: $\boldsymbol{u}_r\big|_\Gamma=\text{const}$ or $\frac{\partial \boldsymbol{u}_r}{\partial y}\Big|_\Gamma=0$ $\Big(\frac{\partial \boldsymbol{u}_r}{\partial x}\Big|_\Gamma=0\Big)$, or $T\big|_\Gamma=\text{const}$ or $\frac{\partial T}{\partial y}\Big|_\Gamma=0$ $\Big(\frac{\partial T}{\partial x}\Big|_\Gamma=0\Big)$. Approximation of each type of the boundary conditions in both cases is similar

and is carried out according to the above described technique, except for the integration with respect to half the control volume when discretizing the first type conditions.

To calculate the velocity fields and consistent with them the pressure field and the parameter field Q, exactly satisfying the continuity equation, we use the iterative algorithm SIMPLE, requiring adaptation to a two-velocity hydrodynamic model, due to the presence in the equations of motion of the parameter Q, which is the analog to the second pressure.

In the transition to a new time step, the initial assumption of the approximate the pressure field values P^* and the parameter field Q^* is made, their true values being determined by the correction values P' and Q':

$$P = P^* + P', \qquad Q = Q^* + Q'. \tag{19}$$

In a similar manner we introduce corrections for the velocity vector components:

$$u_{rx} = u^*_{rx} + u'_{rx}, \qquad u_{ry} = u^*_{ry} + u'_{ry}. \tag{20}$$

Further, by subtracting the exact and approximate discrete analogs to the equations of motion and rejecting a number of terms that may be admissible in using the algorithm SIMPLE, we introduce the following expressions for corrections:

$$u'_{rx;i+1/2,j} = \frac{\Delta y}{a_{r;i+1/2,j}} \frac{\rho_{r;i+1/2,j}}{\rho_{i+1/2,j}} (P'_{i,j} - P'_{i+1,j}) + (-1)^r \frac{\Delta y}{a_{r;i+1/2,j}} \frac{\rho_{1;i+1/2,j}\rho_{2;i+1/2,j}}{\rho_{i+1/2,j}} (Q'_{i,j} - Q'_{i+1,j}), \tag{21}$$

$$u'_{ry;i,j+1/2} = \frac{\Delta x}{a_{r;i,j+1/2}} \frac{\rho_{r;i,j+1/2}}{\rho_{i,j+1/2}} (P'_{i,j} - P'_{i,j+1}) + (-1)^r \frac{\Delta x}{a_{r;i,j+1/2}} \frac{\rho_{1;i,j+1/2}\rho_{2;i,j+1/2}}{\rho_{i,j+1/2}} (Q'_{i,j} - Q'_{i,j+1}). \tag{22}$$

Substituting (20)–(22) into the discrete analogs of continuity equations (18) leads to a linear algebraic equation for calculating the corrections for the pressure field and the parameter Q (values of linear coefficients are not given here, because they are cumbersome and uninformative):

$$\begin{aligned} A_{i,j}P'_{i,j} + B_{i,j}Q'_{i,j} = {} & A_{i+1,j}P'_{i+1,j} + B_{i+1,j}Q'_{i+1,j} + A_{i-1,j}P'_{i-1,j} + \\ & B_{i-1,j}Q'_{i-1,j} + A_{i,j+1}P'_{i,j+1} + B_{i,j+1}Q'_{i,j+1} + \\ & A_{i,j-1}P'_{i,j-1} + B_{i,j-1}Q'_{i,j-1} + E_{i,j}, \end{aligned}$$

where $E_{i,j}$ comprises the residuals of the equations of continuity and is a necessary indicator to the convergence of the iterative process.

A stepwise scheme of applying the algorithm is as follows:

1. The assumption of the first approximation of the pressure field P^* and the parameter Q^*.
2. The solution to discrete analogs of equations of motion (18) to find approximate values of the fields of the components of the vector velocities u^*_{rx} and u^*_{ry}.
3. Finding the field of correcting the pressure P' and the correction parameter Q' from the solution of the correcting equation.
4. Calculation of a new value of the pressure field P and the parameter Q by formulas (19).
5. Calculation of new values for the velocity field components u_{rx}, u_{ry} by formula (20).
6. Solution of the discrete analog to the entropy balance equation.
7. Recalculation of the density and the temperature fields through the equation of state with the new values of the pressure and the entropy fields.
8. Representation of the corrected pressure field P and the parameter Q as new values P^* and Q^*, repeating the procedure up to the convergence of the iterative process.

To resolve the resulting discrete analogs to the governing equations of the model, we use a combination of the direct method of three-point sweep with an iterative Gauss–Seidel method which is the method of alternating directions with a supplementary modification to solve a complex structured system of equations for correcting the pressure and the parameter.

3. Numerical results

The paper presents the results of numerical modeling of non-stationary hydrodynamic problems of the two-velocity granular medium. To verify the mathematical model, we have considered a classical problem of convection in a rectangular cavity with different temperatures on the lateral boundaries [11–13] as applied to the two-velocity hydrodynamics. The geometry of the computational domain is shown in Figure 2 (in Figures 2, 3, 9 below the horizontal axis corresponds to the variable x, the vertical axis being y). At the boundaries, the non-flow and adhesion conditions are set. The temperature at the initial time was assumed to be the same in the domain, except for the left boundary, where the temperature rise by was observed. Figure 2 is an example illustrating a difference in the temperature distribution when attaining a stationary state of convection in the two-fluid medium with and without consideration of the interfacial friction and viscosity of the phases.

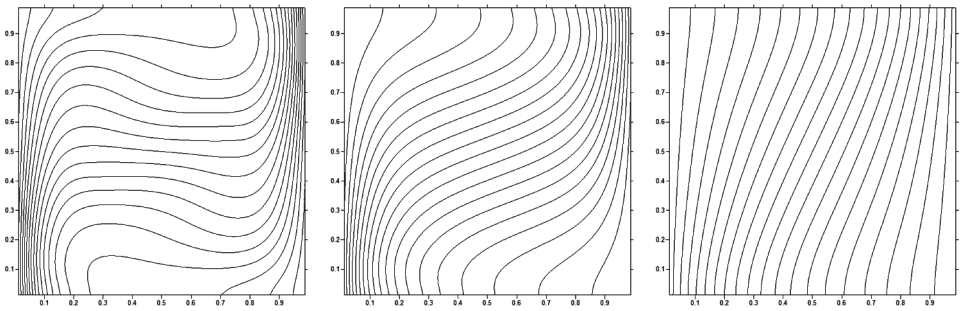

Figure 2. The two-velocity model of the temperature convection profiles in the two-phase sandstone-water media without ($b = 0$) and with ($b = 10^{-2}$, 10^{-1}) interfacial friction

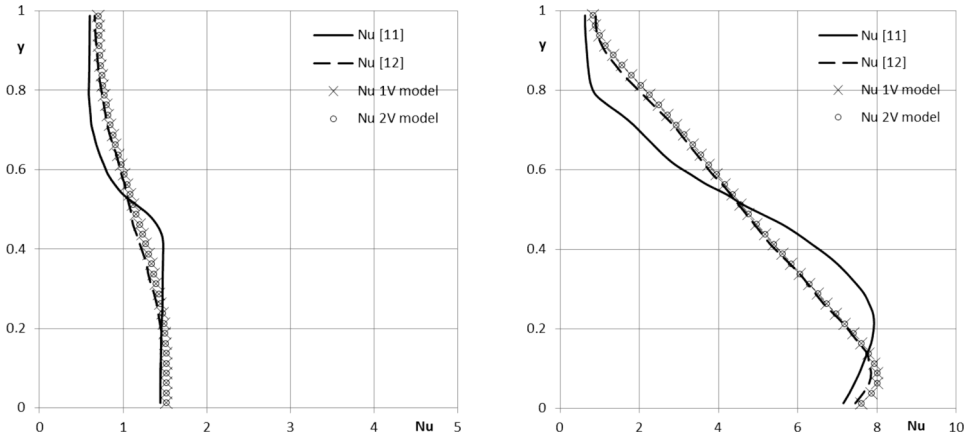

Figure 3. The distribution of the Nusselt number Nu on the left hot boundary for $\mathrm{Ra} = 10^3$, 10^5: crosses denote the results of the one-velocity model [14], circles denote the results of the two-velocity model with identical component parameters, the solid line denotes the data taken from [11–13], the dashed line denotes the data taken from [11–13]

The verification of the model was carried out on the one-velocity model [14] and compared to the standard reference calculations. With the coincidence of properties of the phases that make up a two-velocity medium a limit transition to the one-fluid model is performed, which is reflected in Figure 3, which shows the profiles of the local Nusselt number. The latter characterizes the relationship between the intensity of heat transfer by convection and conduction, on the left hot boundary for different Rayleigh numbers for the two-velocity model under consideration, and one-velocity models.

The data shown in Figure 3 demonstrate a good agreement of the values of the Nusselt number on a hot wall obtained for the two-velocity model

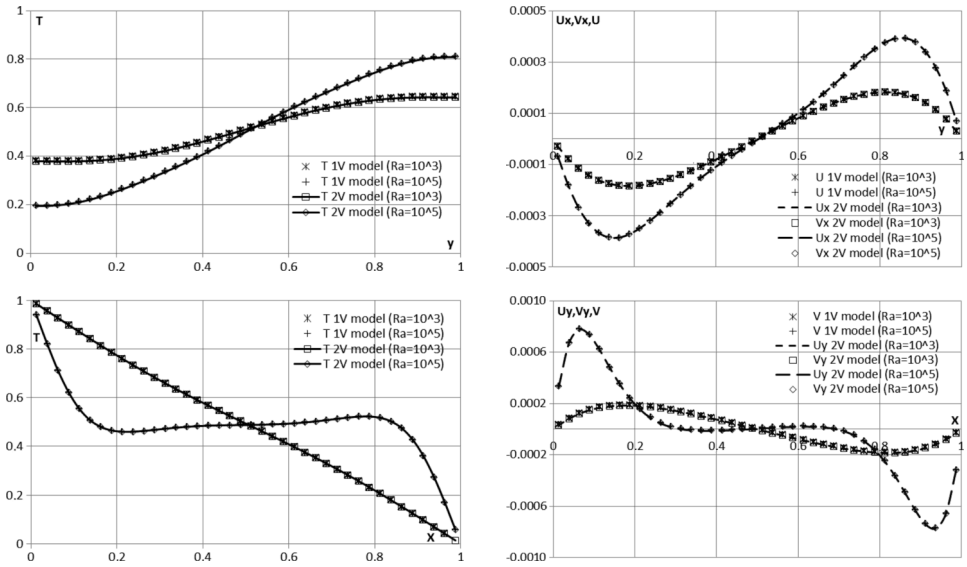

Figure 4. The temperature profiles and the velocity components along the central vertical and horizontal cross-sections of the computational domain for the one-velocity (1V) model and for the two-velocity (2V) model with the same component properties with different values of the Rayleigh number ($\mathrm{Ra} = 10^3, 10^5$)

with the same component, and those obtained according to the benchmark calculations [11–13] and the results of calculations within one-velocity model [10] for a convective flow characterized by different Rayleigh numbers. The corresponding velocity components and temperature profiles along the central vertical and horizontal cross-sections of the computational domain for the two-velocity model with identical component parameters and the one-velocity model are shown in Figure 4.

Examples of convective flows of a two-phase medium with different properties of the phases (water-saturated sandstone) are given in Figure 5. The figures demonstrate a strong influence of the interphase friction on the character of a convective flow and a weak influence on the temperature distribution.

In other words, the interphase friction does not practically affect the heat transfer mechanism. A strong dependence on the Rayleigh number observed in Figure 3 is not the case with the analogous variation of the Darcy number for the two-fluid mixture (Figure 6).

The interaction of phases is clearly observed also in the problem of the pressure flow through the canal. The computational domain is a vertical rectangular canal, on whose lateral boundaries the non-flow and the adhesion conditions were accepted. The upper boundary was assumed to be free. In the central part of the lower boundary, phase 2 was pumped. Initially, the two-fluid medium in the canal was at rest.

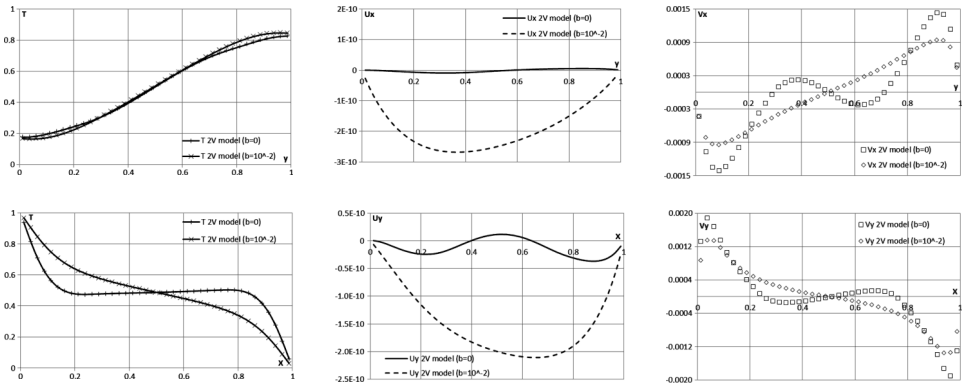

Figure 5. The temperature profiles and the velocity components along the central vertical and horizontal cross-sections of the domain for the Rayleigh number $\mathrm{Ra}_2 = 10^7$ without ($b = 0$) and with ($b = 10^{-2}$) interfacial friction. This is the case of a free convection in a two-phase medium sandstone/water

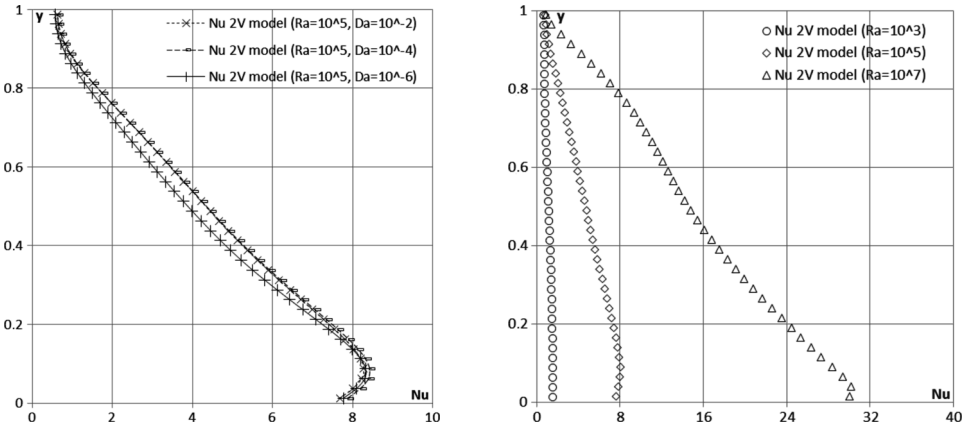

Figure 6. The values of the Nusselt number on the left hot boundary for various Rayleigh numbers (left, $\mathrm{Ra} = 10^3$, 10^5, 10^7) and the Darcy numbers (right, $\mathrm{Da} = 10^{-2}$, 10^{-4}, 10^{-6}). Two-velocity model with components corresponding to sandstone saturated with water

The verification results of the one-velocity model for a viscous compressible fluid are shown in Figure 7. Properties of the phases of a two-fluid medium were chosen to be identical and corresponding to water parameters. There is a good agreement between the results.

Examples of the results of the simulation of the Poiseuille flow in the two-phase medium canal with different properties of the phases (water-saturated sandstone) are presented in Figures 8 and 9.

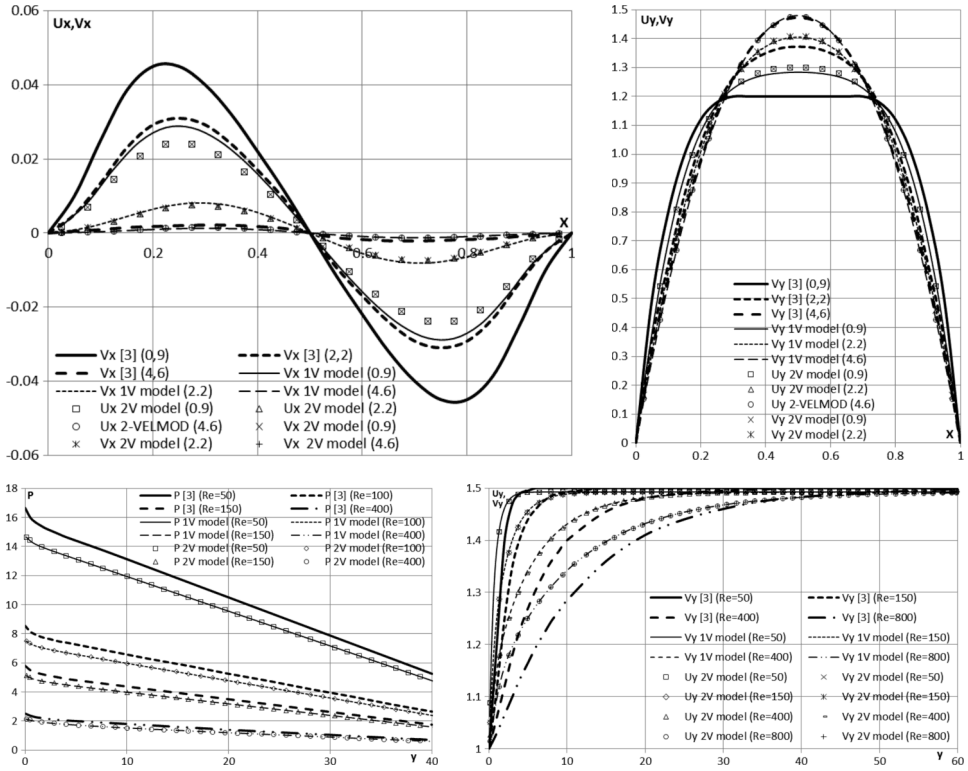

Figure 7. The pressure and vertical velocity component profiles along the central vertical section with different Reynolds numbers (Re = 50, 100, 150, 400, 800) and the velocity vectors components along three horizontal sections ($y = 0.9$, 2.2, 4.6) with the Reynolds number Re = 100 for the one-velocity (1V) model, the two-velocity (2V) model and the results from [15]

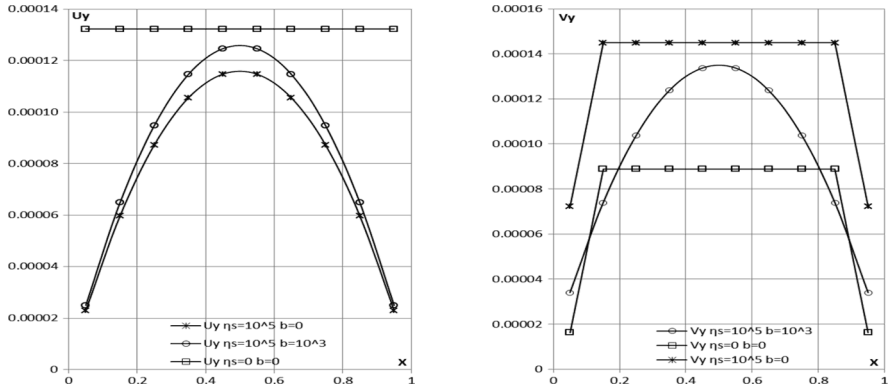

Figure 8. The vertical components of the phase velocity profiles along the central cross-section along the canal without ($\eta_s = 0$) and with ($\eta_s = 10^5$) viscosity of the second phase and without ($b = 0$) and with ($b = 10^3$) interfacial friction. The two-phase medium is a sandstone saturated with water

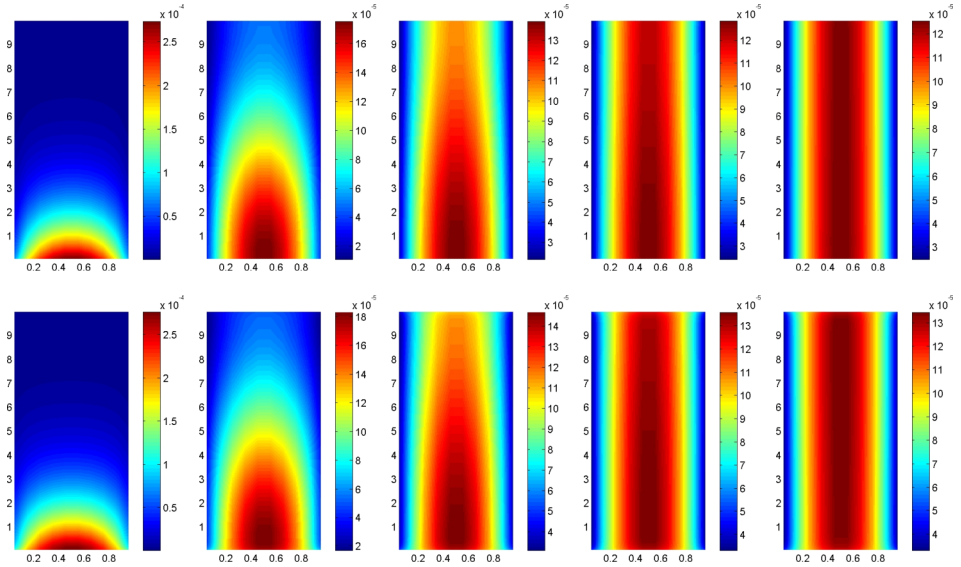

Figure 9. The fields of vertical components u_y (top) and v_y (bottom) of the phase velocities at different time instants. The two-phase medium is a water-saturated sandstone

4. Conclusion

Thus, in this paper the thermodynamically consistent model of the dynamics of the two-velocity two-fluid media without phase pressure equilibrium, whose numerical implementation is based on the control volume method, is proposed. The model obtained allows us to study nonlinear processes of heat and mass transfer in heterophase media in a wide range of characteristic times.

References

[1] Landau L.D., Lifshitz E.M. Course of Theoretical Physics, Fluid Mechanics. — Pergamon Press, 1987.

[2] Blohin A.M., Dorovsky V.N. Mathematical Modelling in the Theory of Multivelocity Continuum. — Nova Science Publishing Incorporation, 1995.

[3] Dorovsky V.N. Mathematical models of two-velocity media // Mathematical and Computer Modelling. — 1995. — Vol. 21, No. 7. — P. 17–28.

[4] Dorovsky V.N., Perepechko Yu.V. Mathematical models of two-velocity media. Part II // Mathematical and Computer Modelling. — 1996. — Vol. 24, No. 10. — P. 69–80.

[5] Dorovsky V.N., Perepechko Yu.V. Theory of partial melt // Geology and Geophysics. — 1989. — Vol. 9. — P. 56–64 (In Russian).

[6] Dorovsky V.N., Perepechko Yu.V. A hydrodynamic model for a solution in fracture-porous media // Geology and Geophysics. — 1996. — Iss. 9. — P. 123–134 (In Russian).

[7] Dorovsky V.N., Perepechko Yu.V., Fedorov A.I. The Stoneley waves in the Biot–Johnson theory and continual filtration theory // Russian Geology and Geophysics. — 2012. — Vol. 53. — P. 621–630.

[8] Winkler K.W., Liu H.L., Johnson D.L. Permeability and borehole Stoneley waves: Comparison between experiment and theory // Geophys. — 1989. — Vol. 54. — P. 66–75.

[9] Patankar S.V. Numerical Heat Transfer and Fluid Flow. — Taylor & Francis Group., 1980.

[10] Perepechko Yu.V., Sorokin K.E. Two-velocity dynamics of compressible heterogeneous media // Natural and Technical Sciences. — 2012. — No. 5. — P. 40–48.

[11] Wan D.C., Patnaik B.S.V., Wei G.W. A new benchmark quality solution for the buoyancy-driven cavity by discrete singular convolution // Numerical Heat Transfer. Part B. — 2001. — Vol. 40. — P. 199–288.

[12] Massarotti N., Nithiarasu P., Zienkiewicz O.C. Characteristic-Based-Split (CBS) algorithm for incompressible flow problems with heat transfer // Int. J. Numer. Meth. Heat Fluid Flow. — 1998. — Vol. 8. — P. 969–990.

[13] Manzari M.T. An explicit finite element algorithm for convective heat transfer problems // Int. J. Numer. Meth. Heat Fluid Flow. — 1999. — Vol. 9. — P. 860–877.

[14] Perepechko Yu.V., Sorokin K.E., Imomnazarov Kh.Kh. Numerical simulation of the free convection in a viscous compressible fluid // Bull. Novosibirsk Comp. Center. Ser. Mathematical Modeling in Geophysics. — Novosibirsk, 2011. — Iss. 14. — P. 59–64.

[15] Buryatsky E.V., Kostin A.G., Nikiforovich E.I., Rozumnyuk Ch.N. A method of numerical solution of the Navier-Stokes equations in variable velocity-pressure // Applied Mechanics. — 2008. — Vol. 10, No. 2. — P. 13–23 (In Russian).